EFFECT OF DIFFERENT BANDWIDTHS FOR THE DETECTION OF EXTENDED TARGETS IN REVERBERATION

S.Ries and H. Schmidt-Schierhorn
Atlas Elektronik GmbH, Sebaldsbrücker Heerstraße 235,
W-2800 Bremen, Germany

Abstract In this paper, firstly the theoretical background of bandwidth effects on detection in noise and reverberation is presented in some detail, and secondly the relevant results of sea trials with a low frequency active sonar are shown and commented upon.

If a frequency-modulated (FM) signal is processed by the optimum processor in the Neyman-Pearson sense, which is a matched filter followed by a square-law detector and an incoherent integrator, the statistical theory of signal detection predicts that, for an extended target in reverberation, a larger bandwidth of the FM signal will result in improved detection quality. For an extended target in noise, the situation is more complicated and depends on the signal-to-noise ratio. Of course, the validity of the classical theory depends also on boundary conditions such as temporal coherence of the received signal and the time-bandwidth product of the FM in relation to the relative target velocity. Therefore, an alternative signal processing scheme is presented here which is equivalent to the classical processor described above, but has the advantage of being much more robust if the coherence degrades or the target velocity inceases higher. Further, it is shown that the bandwidth effect is valid also for normalized detection using several specific normalizers. This is important because a digital display requires normalized data with reduced dynamic range. Also, it is often desirable to obtain a constant false alarm rate which can be obtained by suitable normalization. The relevant experimental data was collected during sea trials with an activated low frequency towed array. Typical results are shown and discussed in connection with the theoretical investigations.

1 Introduction

The first aim of this paper is to investigate two different signal processing methods for the detection of extended targets in noise and reverberation: the matched filter with post detection integration, and the split-spectrum-averaging processor. The

transmitted waveform is typically a wide-band frequency-modulated signal. It is shown by means of a theoretical target model that the two processing methods can, under reasonable assumptions concerning the temporal coherence of the channel, have almost equal detection performance since they generate the same statistics and have equal temporal resolution. The arguments for the split-spectrum processor are based on spectral properties of signal returns from extended targets. The development then makes it possible to study the effect of increased signal bandwidth. The next important step is to include normalization or CFAR-processing. Results with real data are presented, which underline the validity of the theoretical model.

2 Signal Processing for the Detection of Extended Targets

The first signal processor implemented is the matched filter (replica correlator), followed by a square-law device and an integrator. It is well known that, for a linear FM with bandwidth B, the matched filter leads to pulse compression, and the temporal resolution of the compressed signal is 1/B. The integrator is needed, since for optimum detection in the Neyman-Pearson sense the integrator must match the final resolution to the target length. (Note that all figures and calculations are for complex baseband-demodulated signals.)

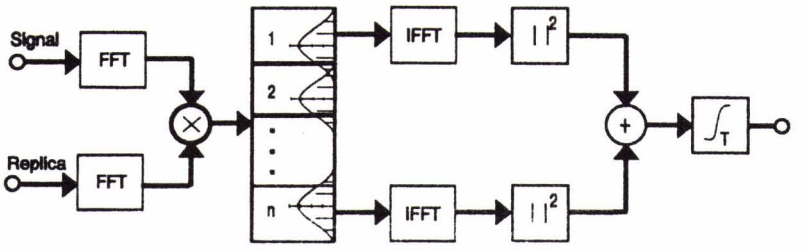

Fig. 2.1: Split-spectrum processor

The second processor considered is the split-spectrum processor from the literature on ultrasonic testing; see [Newhouse et al., 1982]. The main point of this method is that, first, a full correlation is performed by multiplication in the spectral domain, and the result is split into n (possibly windowed and overlapping) frequency cells, which are then transformed back into the time domain, square-law detected, and added (Fig. 2.1). However, it turns out that this is nothing more than a flexible and elegant realisation of a segmented replica correlator with individual replicas that are disjunct in the frequency domain. This processor, the segmented replica correlator with square-law device, delay lines and summation, is shown in Fig. 2.2. Again, if each of the n replicas is a linear FM with bandwidth B/n, pulse compression leading to a resolution of n/B occurs, and hence an integrator might have to be added if

$n/B < T_L$, where T_L denotes the virtual target length in seconds. Therefore, by a suitable choice of bandwidths and integration time, the two processors can achieve the same temporal resolution, matched to the target length.

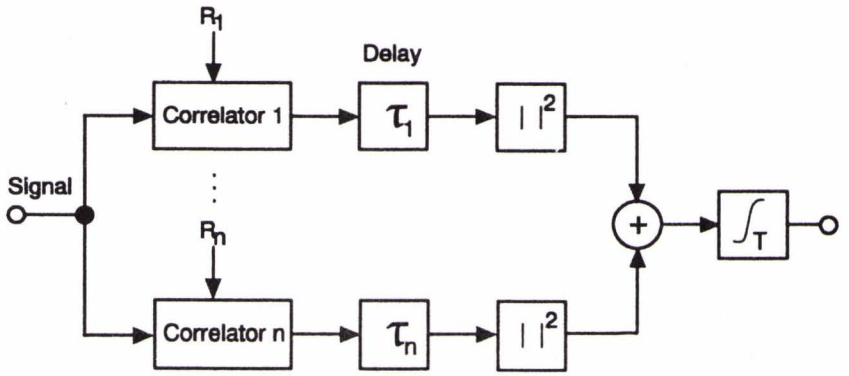

Fig. 2.2: Segmented replica correlator

3 Theoretical Aspects of the Detection Problem

An overview of some theoretical results will be given in this section, the material is classical, see [Proakis, 1989; van Trees, 1971]. First, the target model is presented. The terminology from [van Trees, 1971] is used, so that the definitions do not have to be repeated. The main assumptions are that the target and reverberation can be modelled as zero-mean complex Gaussian processes $b_T(x)$ and $b_R(x)$, respectively, and the signal reflected from the target and the reverberating environment is given by the following (note that capitals denote Fourier transforms and * convolution):

$$a_T(t) = (f * b_T)(t) + (f * b_R)(t) + n(t) \tag{1}$$

Absence of Doppler shift and spread is required in the first step. Their effects will be taken into account later. The noise $n(t)$ is white and Gaussian with average intensity N_0. Further, the range-scattering function of the target is given by

$$s_T(x) = E\{\mid b_T(x) \mid^2\},$$

and the range-scattering function of the reverberation by

$$s_R(x) = E\{\mid b_R(x) \mid^2\},$$

where E denotes the expected value. The Fourier transforms of s_T and s_R, denoted by S_T ans S_R, are the target and reverberation *two-frequency correlation functions.* If the target length in seconds is now T_L, then [van Trees, 1971]

$$S_T(v) \approx 0, \mid v \mid > \frac{1}{T_L} \tag{2}$$

This leads to frequency-selective fading of the target returns, and it means that frequencies separated by more than $\approx 1/T_L$ are statistically independent. If the length of the reverberation zone is greater than the target, the reverberation component will also be independent in frequency increments $\mid \delta v \mid > 1/T_L$. If the emitted signal $f(t)$ with bandwidth B is chosen now such that it can be decomposed into n signals, each with bandwidth B/n and equal energy which are disjunct in the frequency domain, such that $B/n \approx 1/T_L$, then the outputs of each of the channels of the split-spectrum processor are independent random variables.

On the other hand, with this target model, the analysis of the matched filter with incoherent integration leads to the same statistics with the same parameters, as long as the number of integrated independent samples is the same for both processors. The argument is that the first processor sums independent time samples. If the range-scattering function of the reverberation approximately equals a constant power density R_0 (this is the case if returned reverberation can be modelled as a weak-sense stationary process, the power spectrum of which has the same shape as the spectrum of the emitted signal), then the signal-to-reverberation ratio in the reverberation-limited case is equal for each frequency cell and independent of the signal bandwidth B, as long as $B/n > 1/T_L$. In contrast to this, the signal-to-noise ratio in the noise-limited case is inversely proportional to the signal bandwidth in this case. This leads to bandwidth effects for the detection of extended targets, wich will be discussed in the next sections.

It should be mentioned that there are also results for the detection probabilities for correlated Rayleigh targets [Kantner, 1986; Hellstrom, 1992]. However, in practice it is very difficult to make any reasonable assumption about the correlation of unknown targets. Therefore, we choose here the hypothesis of uncorrelated target time or frequency cells.

3.1 Bandwidth Effects for (N,N) Targets

If the target is divided by either of the two processors from chapter 1 into N (time-domain or frequency-domain) independent Rayleigh cells, then each of the N square-law envelope detected samples has the probability density function (pdf)

$$p_z(z) = C exp(-Cz) \tag{3}$$

where

$$C = \frac{1}{1 + \overline{SNR}} \tag{4}$$

and the average SNR $\overline{SNR}$ per target cell is

$$\frac{\overline{E}}{R_0} \tag{5}$$

in the reverberation limited case, and

$$\frac{\overline{E}}{NN_0} \tag{6}$$

in the noise-limited case; $\overline{E}$ is the average reflected target energy before matched filtering or frequency windowing. This target model is the (N,N) or fully populated target. It is further assumed that a bandwidth increase for this kind of target leads to an increase of N; if this is not true, the model described in the next section should be considered.

The statistics of the sum of N independent square-law detected samples is given by the well-known central chi-square distribution [Whalen, 1971; van der Spek, 1971] with the corresponding signal-to-noise or reverberation ratio from (5) or (6), respectively. The detection probability P_d as a function of the threshold d is then given by

$$P_d = exp(-Cd) \sum_{j=0}^{N-1} \frac{Cd^j}{j!} , \tag{7}$$

and the false alarm rate, i.e. P_d for $\overline{SNR} = 0$, by

$$P_{fa} = exp(-d) \sum_{j=0}^{N-1} \frac{d^j}{j!} . \tag{8}$$

For this statistics at the detector output, there are extensive results for the detection performance, including bandwidth (resolution) effects; see [van der Spek, 1971; van der Spek, 1972]. Note that the number of independent samples is proportional to resolution, or bandwidth. The results shown here and in the next sections underline the importance of these results and their generalization.

For the (N,N) target, following the arguments from [van der Spek, 1972], the influence of resolution or bandwidth on detection quality can be roughly characterized as follows: their increase increases the number of integrated independent time or frequency samples. This leads to different effects in the noise-limited and reverberation-limited cases, since the signal-to-noise ratio behaves in a different way.

-In the noise-limited case, typically no more than three samples from the target should be integrated, since we then have the change from fluctuation gain to detector or integration loss; this is illustrated in Fig. 3.1. for a false alarm probability of 10^{-3}. Note that a negative loss is a gain.

-In the reverberation-limited case, the resolution or bandwidth should be increased as long as the model assumptions remain valid, as can be seen from Fig. 3.2 for a false alarm probability of 10^{-3}.

Now, the practical importance of the equal detection quality of the two processors is as follows: if the Doppler spread in the medium increases, the full replica correlator, which has the advantage of allowing a high target resolution, which might be desirable for classification purposes, will begin to suffer and will finally fail if the coherence time, which is given by the inverse of the Doppler spread bandwidth [Proakis, 1989], becomes shorter than the pulse duration. The segmented replica correlator is more robust, since the duration of the individual replicas is much shorter than the pulse duration T, and the coherence time required only has to be adapted to allow coherent processing of the segments. Therefore, if it is suspected that Doppler

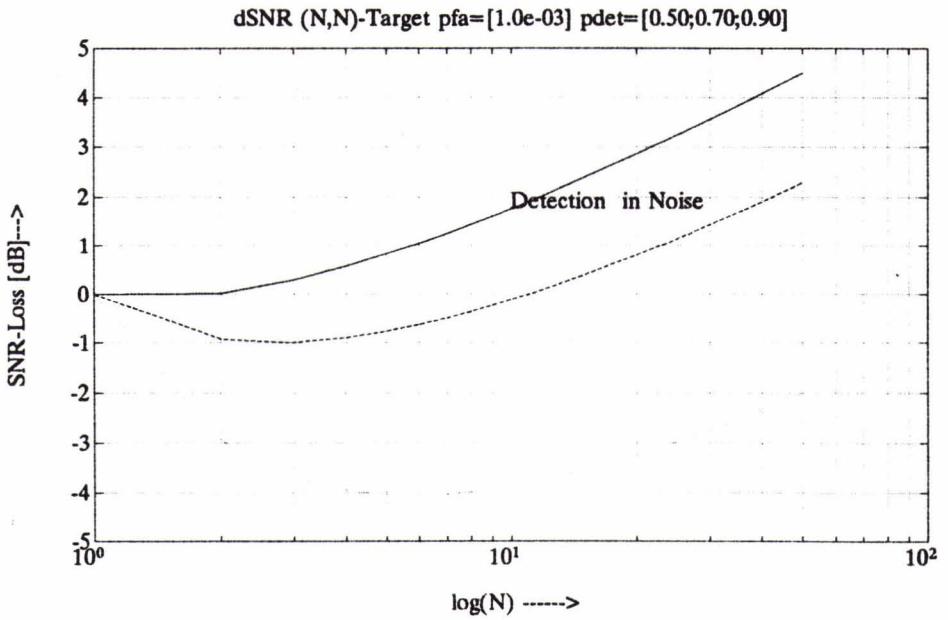

Fig. 3.1: (N,N) Target in Noise

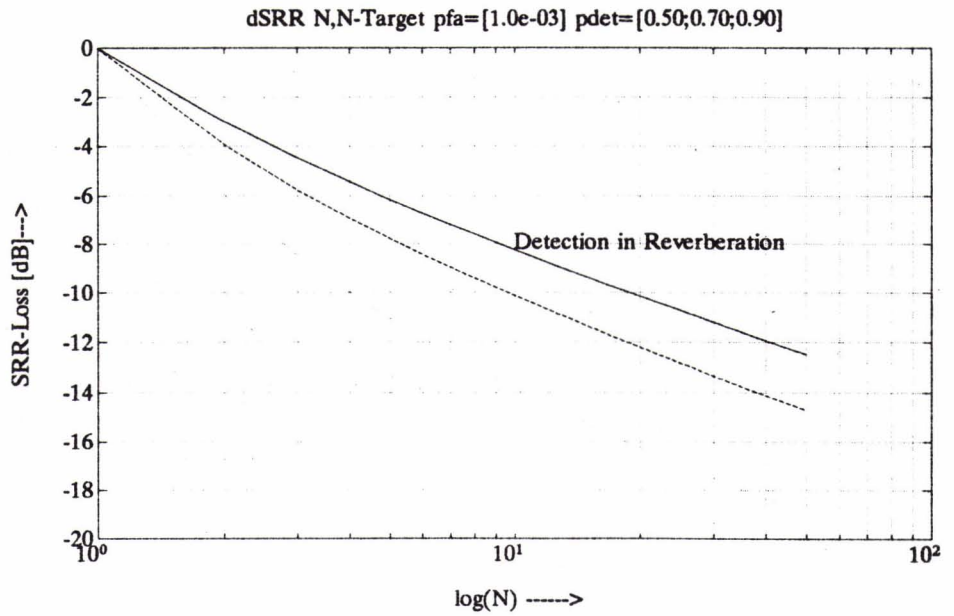

Fig. 3.2: (N,N) Target in Reverberation

spread may cause problems, a segmented replica correlator should be used. Also, it is known that the tolerance concerning Doppler shift of linear FM signals is inversely proportional to its time-bandwidth product. The condition

$$BT < \frac{c}{v} \tag{9}$$

where c is the speed of sound and v the target velocity. If this condition is violated, coherent processing degrades rapidly. Therefore, the split-spectrum processor is also more robust in this respect, because the time-bandwidth product of the pulse segments is of course smaller than that of the original signal. Since the split-spectrum processor contains both methods, and since they are based on the same type of pulse, a software implementation makes it possible to choose the processor adapted to the environmental conditions.

3.2 Bandwidth Effects for Sparse Targets

In the foregoing section, the influence of bandwidth on the detection of a fully populated, i.e. (N,N) target, was recalled. Now, the perhaps more realistic case of a sparse target, or (N,K) target, is investigated. An (N,K) target is partitioned into N cells, K of which are Rayleigh cells which reflect the transmitted signal such that the average energy per cell in the receiver (after matched filtering) is $\overline{E}/K$. The remaining cells do not reflect. In [van der Spek, 1971], the analytical solution for this problem has been calculated. It can be given in a closed form by complex contour integration, but for evaluation purposes it is better to calculate the detection probability P_d as a function of the threshold d by the integral

$$P_d = 1 - 2\frac{C^k}{\pi}(-1)^{N/2}\int_0^\infty \frac{\sin(\omega d/2)\cos(\omega d/2 + m\arctan(1/\omega) + k\arctan(C/\omega))}{\omega(\omega^2+1)^{m/2}(\omega^2+C^2)^{k/2}}d\omega \tag{10}$$

C means $1/(1+\frac{\overline{E}}{KN_0})$, and $m = N - K$; N_0 is the white noise or reverberation power spectral density. The calculations in [van der Spek, 1971] can also be generalized to include different target cell reflectivities, but we shall keep it simple here.

First, detection in noise is considered. Increase of bandwidth means that the number of target cells N is increased. We assume now and in the following, that the target consists of exactly K discrete reflectors (think of a submarines bow section, stern section and tower). This means that the bandwidth increase does not increase the number of reflecting target cells. The noise level in the samples from the empty cells remains the same; also, the signal-to-noise ratio in the K reflecting cells does not change, because they contain all the target's reflected energy. Therefore, a bandwidth increase in this case means that, from the moment the reflectors are resolved (until then we have an (N,N) target), only more noise samples are added. The effect is a strong immediate reduction in detection performance. This is shown in Figs. 3.3 and 3.4 for a representative example.

In reverberation, again the situation is different. A bandwidth increase means that the reverberation power in the target cells decreases, and the signal-to-

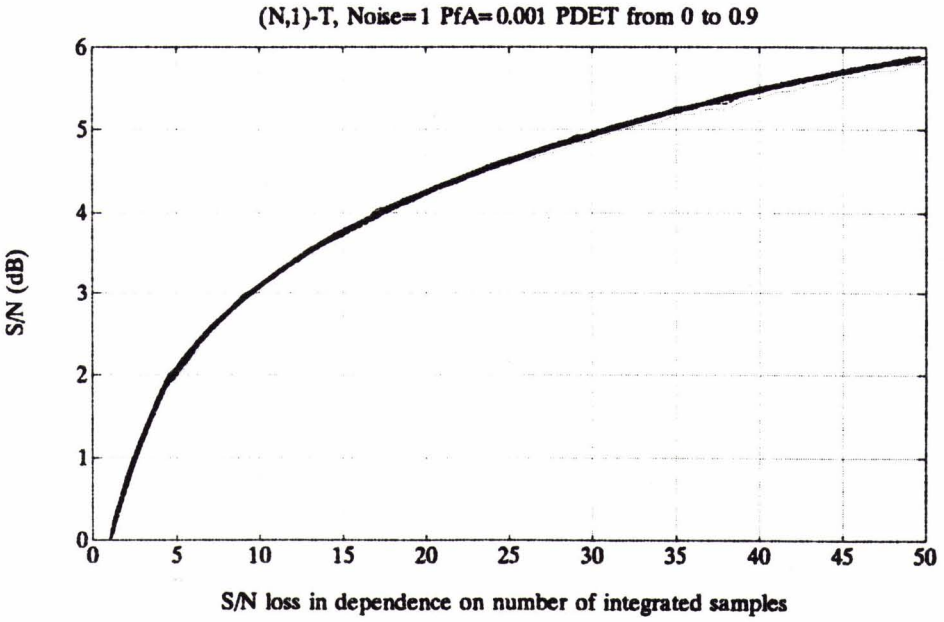

Fig. 3.3: (N,1) Target in Noise, PFA=[0.5 0.7 0.9]

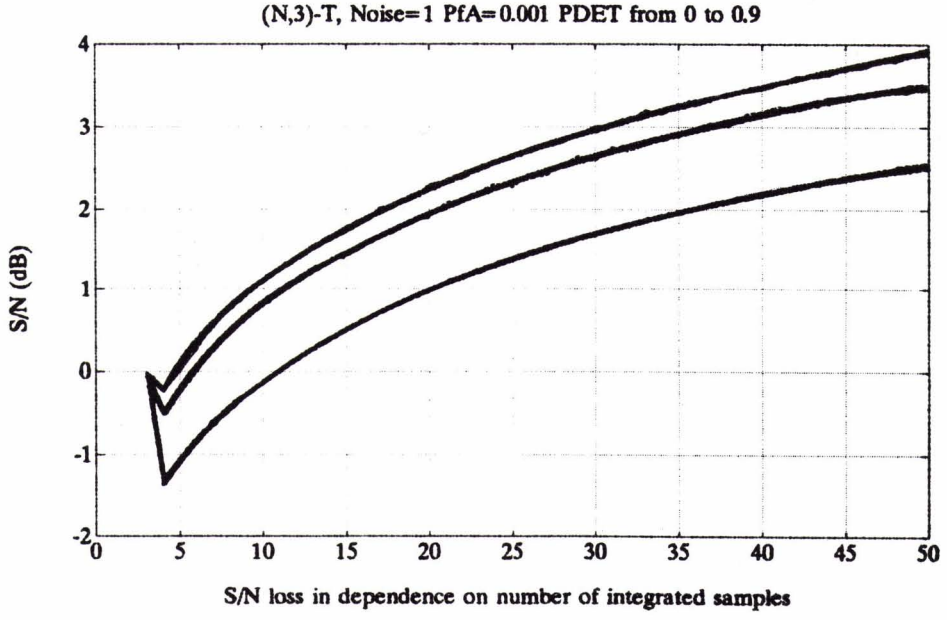

Fig. 3.4: (N,3)-Target in Noise, PFA=[0.5 0.7 0.9]

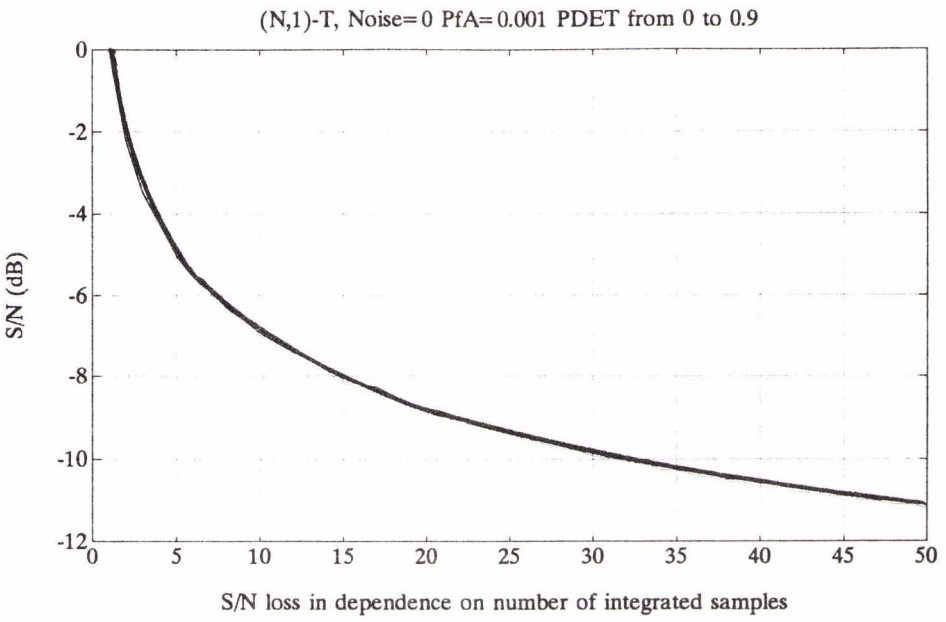

Fig. 3.5: (N,1)-Target in Reverberation, PFA=[0.5 0.7 0.9]

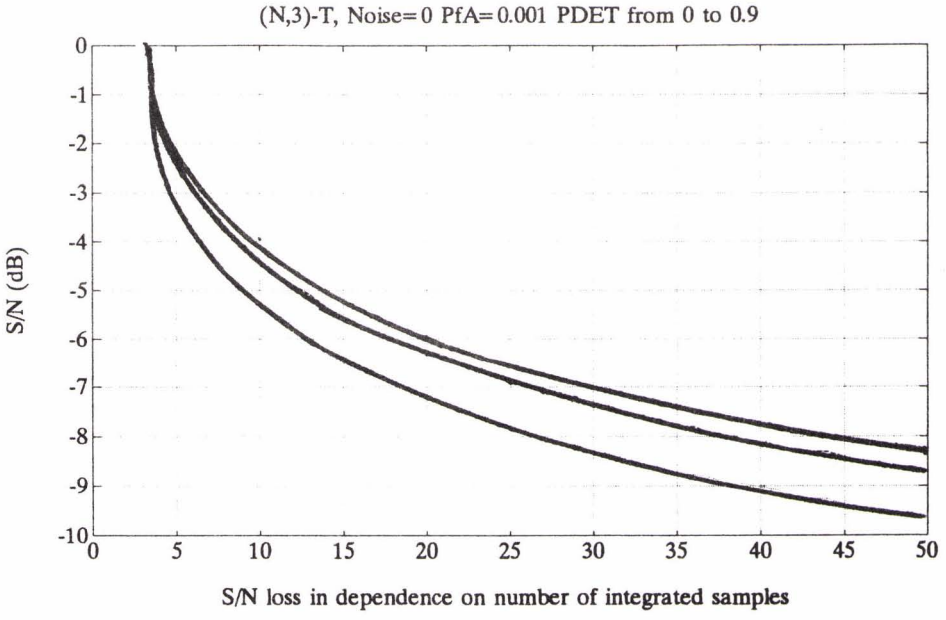

Fig. 3.5: (N,3)-Target in Reverberation, PFA=[0.5 0.7 0.9]

reverberation ratio in the K reflecting cells increases. This means that more bandwidth still leads to improved detection by this suboptimum processor. This is shown in Figs. 3.5. and 3.6. Of course, the gain is not as high as for an (N,N) target, since, especially for small K, we have a severe target mismatch. Compare Figs. 3.2 and Figs. 3.5 and 3.6 in this respect.

So one conclusion is that for a sparse target, the bandwidth effects on the detection in noise and reverberation are even more critical than for a fully populated target.

4 Normalized Detection or CFAR

We are now going to include normalized detection in our considerations. This is very important, because the dynamic range of noise or reverberation has to be accounted for in any practical system, especially if the data is shown on a display, which today still has very reduced dynamic range. However, many classical texts on detection theory make the assumption that the noise variance is known and can therefore be set to 1 [Whalen, 1971; van Trees, 1972].

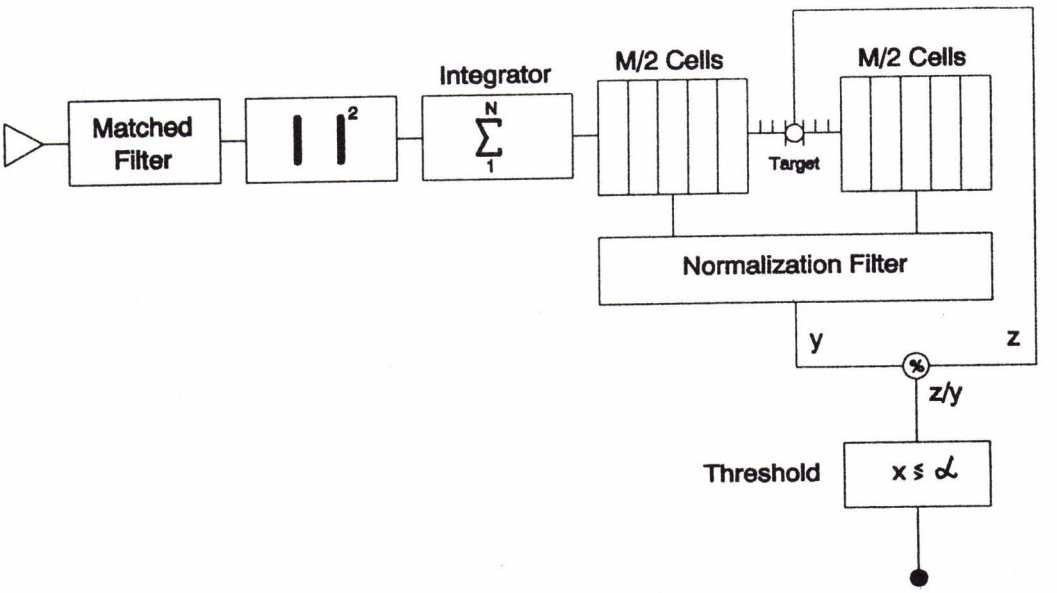

Fig. 4.1: Split-Window Normalization

This is a perfect normalization and is, of course, never true in practice. What always has to be done is to estimate the noise level in the region of interest, and to adjust the detection threshold accordingly in order to obtain a false alarm rate independent of the noise or reverberation level. In publications on radar detection, this is called CFAR (Constant False Alarm Rate) processing. In sonar, it is called normalization.

A very simple derivation of the basic equation goes as follows: In order to set the variance of the noise to 1, the noise signal has to be divided by its variance; this is done by estimating the noise variance and dividing the signal by this estimate. This is often done by means of the well-known split-window estimator, surrounding the cell being tested with two windows (see Fig. 4.1). This also ensures that the occurring random variables of target and noise estimator are independent, which simplifies the calculations.

Now let Z be the random variable produced by the cell under test, with pdf $p_Z(z)$, and Y the random variable produced by the noise estimator, with pdf $p_Y(y)$. We have to form the new random variable $X = Z/Y$, and the detection probability as a function of the threshold d is then

$$P_d = P(X > d) = P(\frac{Z}{Y} > d) = \int_d^\infty p_X(x)dx \tag{11}$$

where $p_X(x) = p_{\frac{Z}{Y}}(x)$. Thus, the pdf of X has to be calculated. Now, if $p_{Z,Y}$ is the joint pdf of Z and Y, then by [Papoulis, 1991]

$$p_{\frac{Z}{Y}}(x) = \int_{-\infty}^\infty p_{Z,Y}(xy, y) \mid y \mid dy \tag{12}$$

Hence, for the detection probability as a function of the threshold α, it follows that

$$P_\alpha = \int_\alpha^\infty dx \int_{-\infty}^\infty p_{Z,Y}(xy, y) \mid y \mid dy = \int_0^\infty dy \int_{\alpha y}^\infty p_{Z,Y}(x, y)dx \tag{13}$$

by a change of variables and assuming that $Y > 0$, which any reasonable noise variance estimator should fulfil. If Z and X are statistically independent (see above), then $p_{Z,Y}(z, y) = p_Z(z)p_Y(y)$, and the final result

$$P_\alpha = \int_0^\infty dy\, p_Y(y) \int_{\alpha y}^\infty p_Z(z)dz \tag{14}$$

follows. This is the fundamental expression for normalized detection. It is often derived in a completely different way [Rohling, 1983; Shor and Levanon, 1991], which in our opinion obscures the fact that we are simply dividing a signal by an estimate of the noise variance. Starting from expression (14), P_α can be evaluated for a number of signal models and noise estimators with the aid of a good integral table. If we assume, as before, a target consisting of independent Rayleigh cells, and if the processor incoherently sums N independent target or noise samples, then the performance of the following normalizers can be obtained [Shor and Levanon, 1991]:

1. Integration of M independent noise or reveberation samples at the processor output (CA-CFAR) as noise estimator; the explicit expression for the detection probability is

$$P_d = \left(1 + \frac{dC}{M}\right)^{-NM} \sum_{j=0}^{j=N-1} \left(1 + \frac{M}{dC}\right)^j \binom{MN - 1 + j}{j} \tag{15}$$

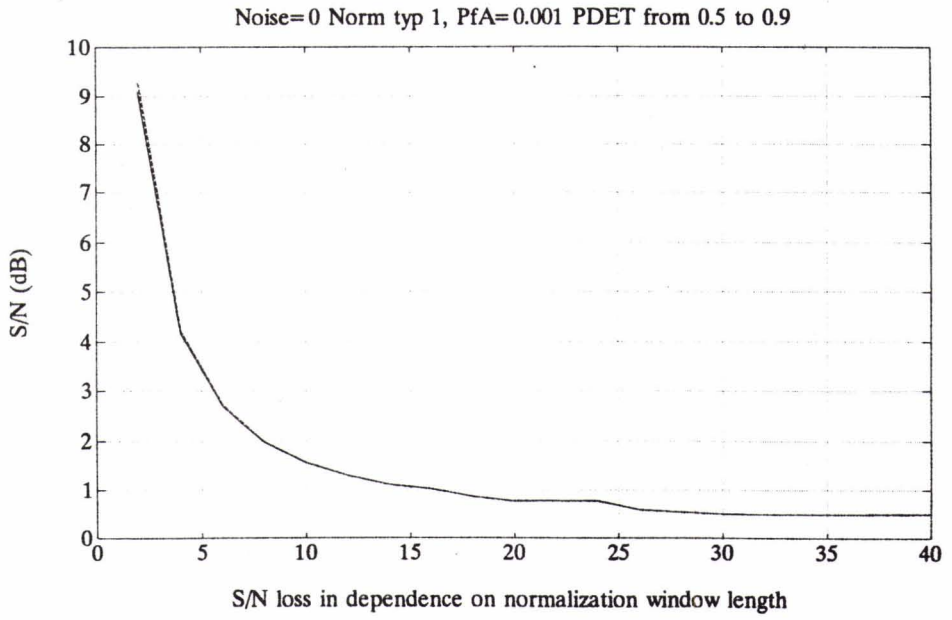

Fig. 4.3: CA-CFAR, N=1, Detection in Reverberation

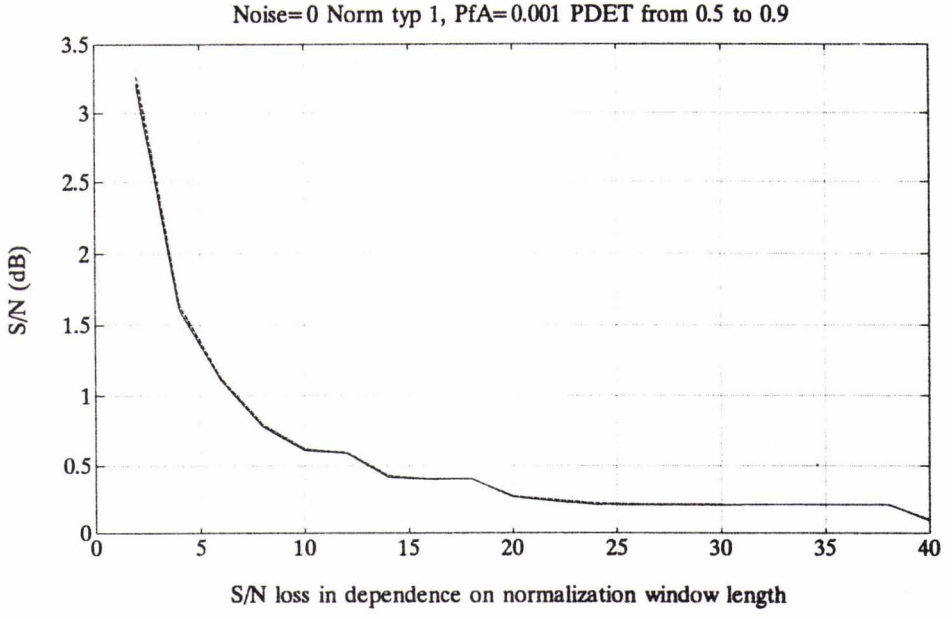

Fig. 4.4: CA-CFAR, N=4, Detection in Reverberation

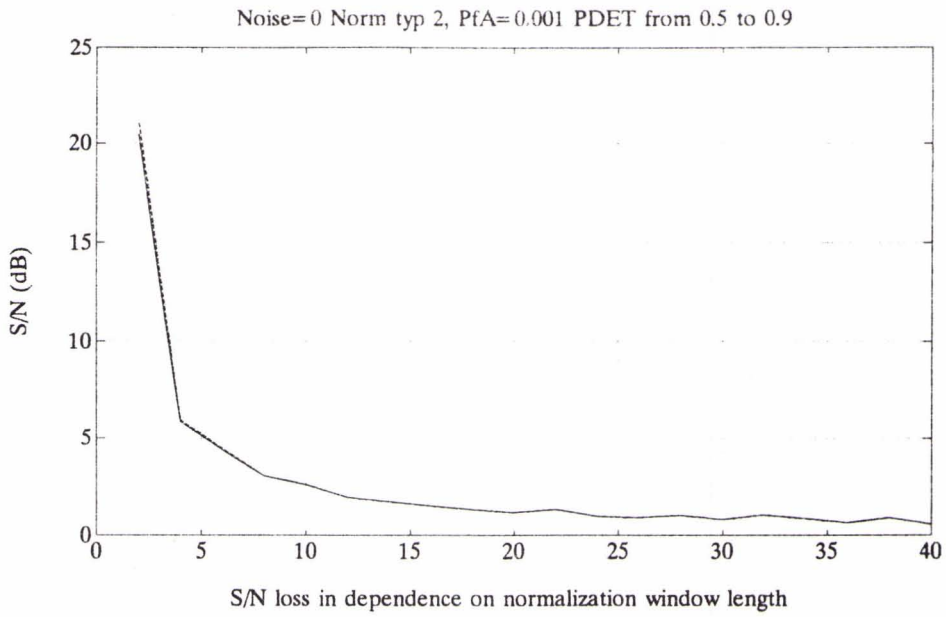

Fig. 4.5: OS-CFAR, N=1, Detection in Reverberation

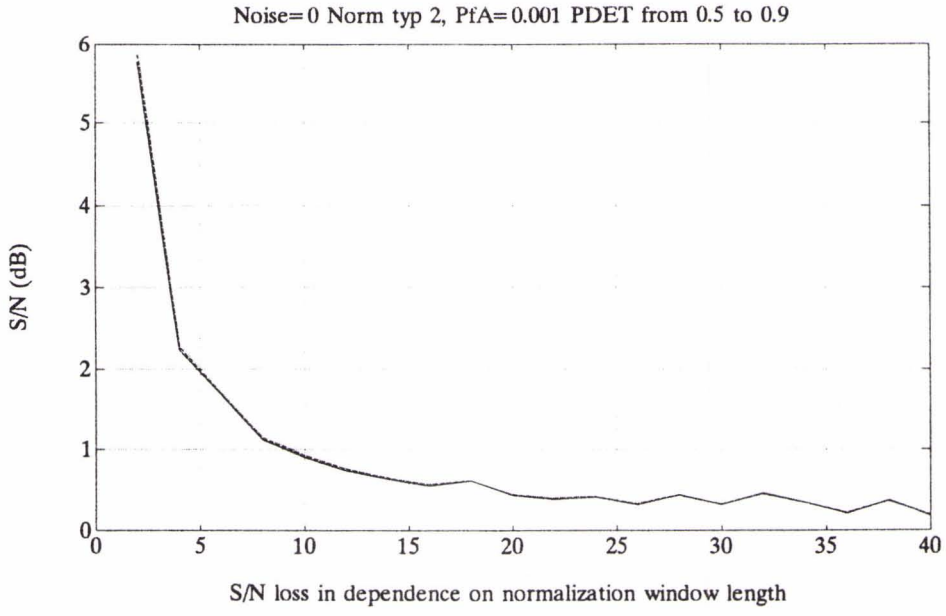

Fig. 4.6: OS-CFAR, N=4, Detection in Reverberation

where $C = 1/(1+\overline{SNR})$, and $\overline{SNR}$ is the average signal-to-noise or signal-to-reverberation ratio of the target cells before integration.

2. Rank-filtering M independent samples of the processor output, i.e. ordering the samples by magnitude and selecting the j-th ranked sample as a noise estimate (OS-CFAR); see [Rohling, 1983; Shor and Levanon, 1991] for details. This kind of normalizer is robust against interference, since this affects only the greatest samples, which should therefore not be selected.

It is clear that the detection probability after normalization is formally lower than before (this is the normalization loss). However, it is the more realistic quantity if normalization is used. Further, the normalization loss can also be calculated in units of extra signal-to-noise needed by the effect of the normalization. The loss becomes quite small if enough independent samples are used for the noise estimation; see Figs. 4.2, 4.3, 4.4 and 4.5 as representative examples.

This also means that the positive bandwidth effects in reverberation are reinforced in normalized detection, since larger bandwidth means that more independent samples can be used for reverberation variance estimation.

As a last point, let us mention that we have derived an expression of the CA-CFAR for a sparse target. However, it is numerically not satisfying and is currently being investigated further. But it should be clear now that similar global effects concerning bandwidth will occur in this case.

5 Experimental Results

The experimental data was recorded in the following way: signals were emitted and collected by a low frequency towed array, and several extended targets were present in a reverberating environment. Among the signals were several wide-band frequency-modulated pulses. Doppler spread induced by the medium and target motion was measured using long CW-signals. The spectral analysis reveals a negligible Doppler spread for the pulse lengths used in the trials. This means that the signals can be processed coherently. This was confirmed, for all data that has been examined, by a direct comparison of the fully coherent matched filter-integrator and the split-spectrum processor, see below.

A broadband spectral analysis of the data considered here shows that the noise level is much lower than the reverberation level, hence we are in the reverberation-limited case.

Frequencies are given from now on in unities of B Hz, and time in unities of A sec.

It is observed (see Figs. 5.1 - 5.2), that coherent and split-spectrum processing are equivalent even for 8A sec/6B Hz pulses and several sets of integration times/frequency window bandwidths. In Figs. 5.3 - 5.4, the fluctuation of the frequency components is shown. The different output channels of the split-spectrum processor are displayed.

In order to get an idea of the bandwidth effect with real data, we have simultaneously emmited a A sec/B Hz and a A sec/4B Hz LFM in different frequency bands. Examples of the results of the two processors for normalized detection are shown in Figs. 5.5 - 5.8. The fluctuations of the target's frequency components are shown in Figs. 5.9. - 5.10. Again, the different output channels of the split-spectrum processor are displayed.

It is observed that this broadband analysis shows that there may be frequencies with high levels and others with very low levels. (This is the frequency selective fading.) This means that a more narrowband pulse can, in the extreme case, completely miss the target or, on the other hand, be very strong. The theory predicts that *on average*, the broadband pulse performs better in reverberation. This statistical effect can, in our opinion, be best assessed in showing both pulses simultaneously on a digital colour display with multiple beams and a ping history in each beam. The human observer then averages a number of target returns, and the advantage of the broadband pulse, in accordance with the theoretical results, is then observed. An example of such a display will be shown at the conference. In Figs. 5.11 - 5.14, an impression of the advantage of the broadband pulse is given by displaying, for the simultaneously emitted pulses, range and beam sections around a target my means of a mesh plot.

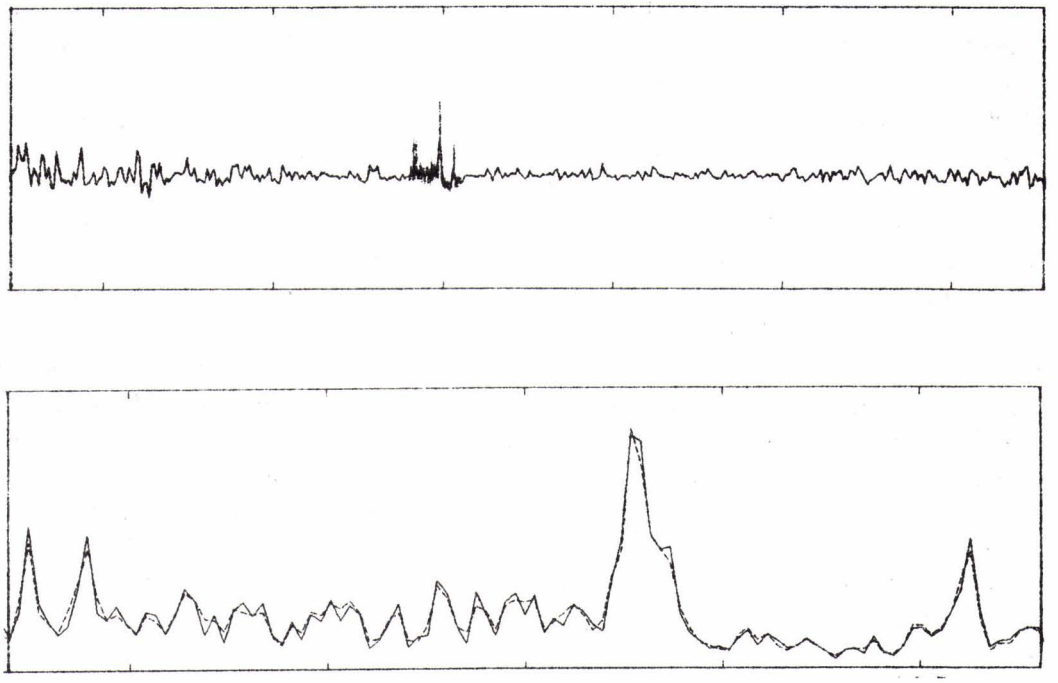

Fig. 5.1: Pulse 8A sec/6B Hz, Matched-Filter-Integrator and Split-Spectrum, Frequency cells B Hz

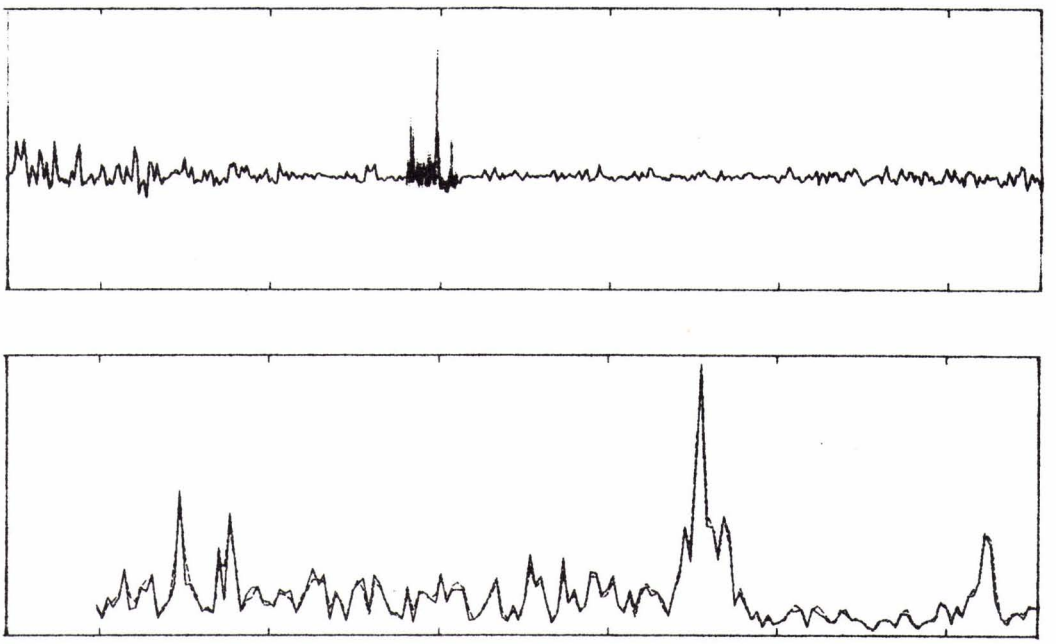

Fig. 5.2: Pulse 8A sec/6B Hz, Matched-Filter-Integrator and Split-Spectrum, Frequency cells 2B Hz

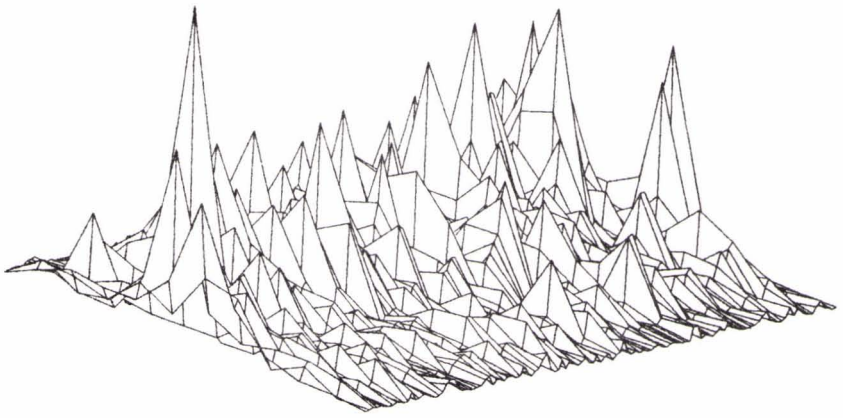

Noise and Reverberation Fluctuation over Frequency

Fig. 5.3: Pulse 8A sec/6B Hz, Frequency cells B Hz

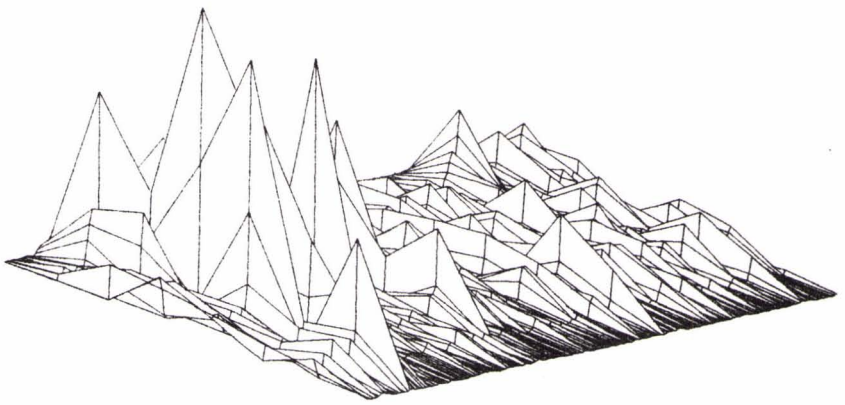

Noise and Reverberation Fluctuation over Frequency

Fig. 5.4: Pulse 8A sec/6B Hz, Frequency cells 2B Hz

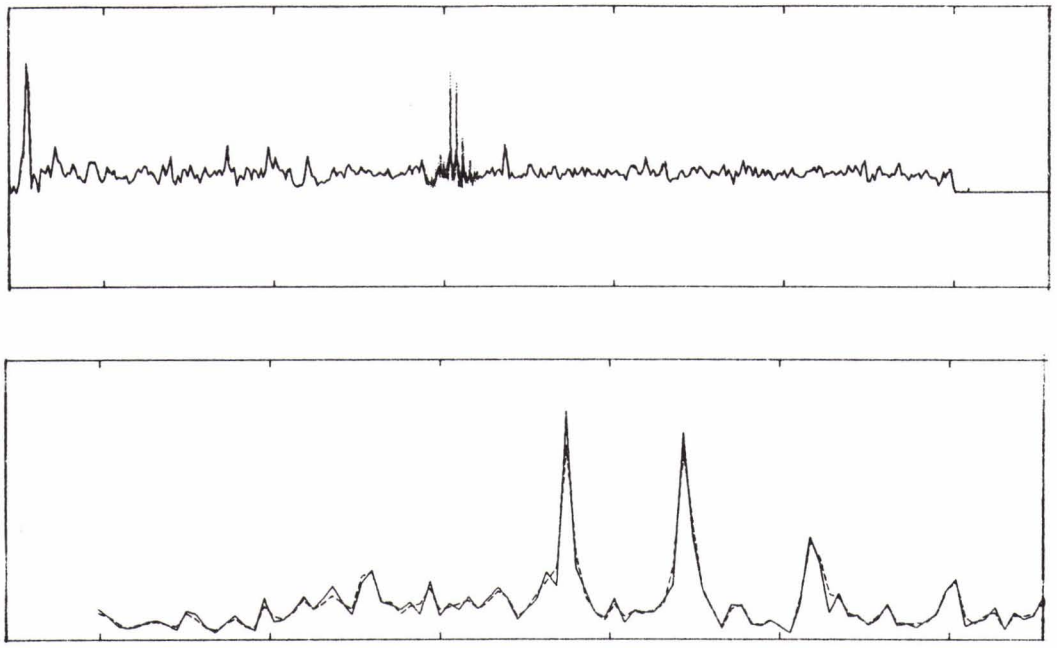

Fig. 5.5: Pulse A sec/4B Hz, Matched-Filter-Integrator and Split-Spectrum, Frequency cells B Hz

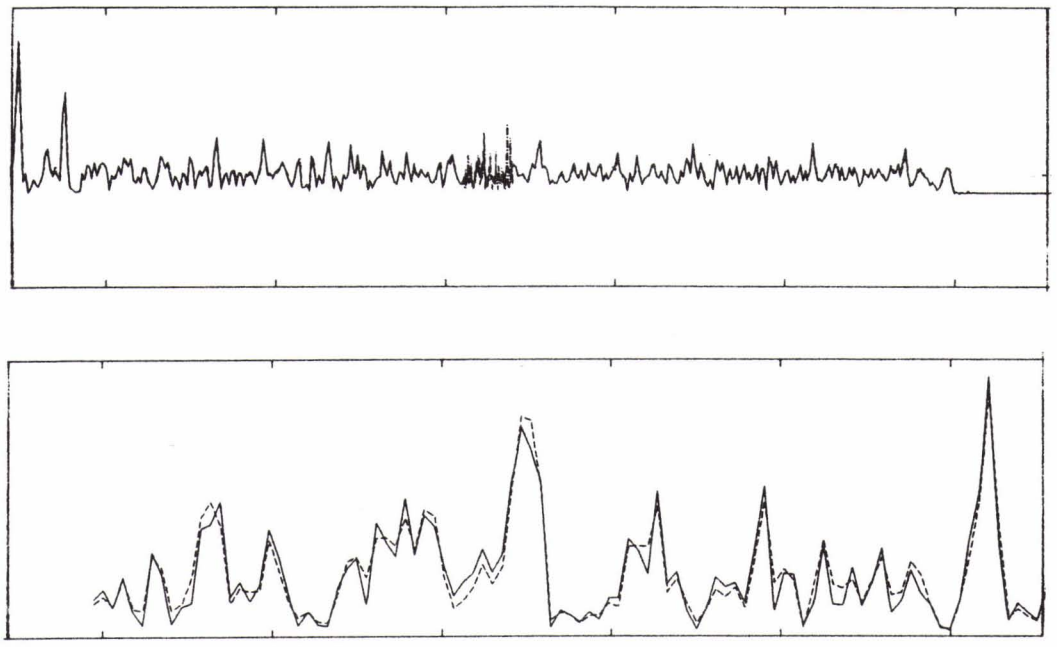

Fig. 5.6: Pulse A sec/B Hz, Matched-Filter

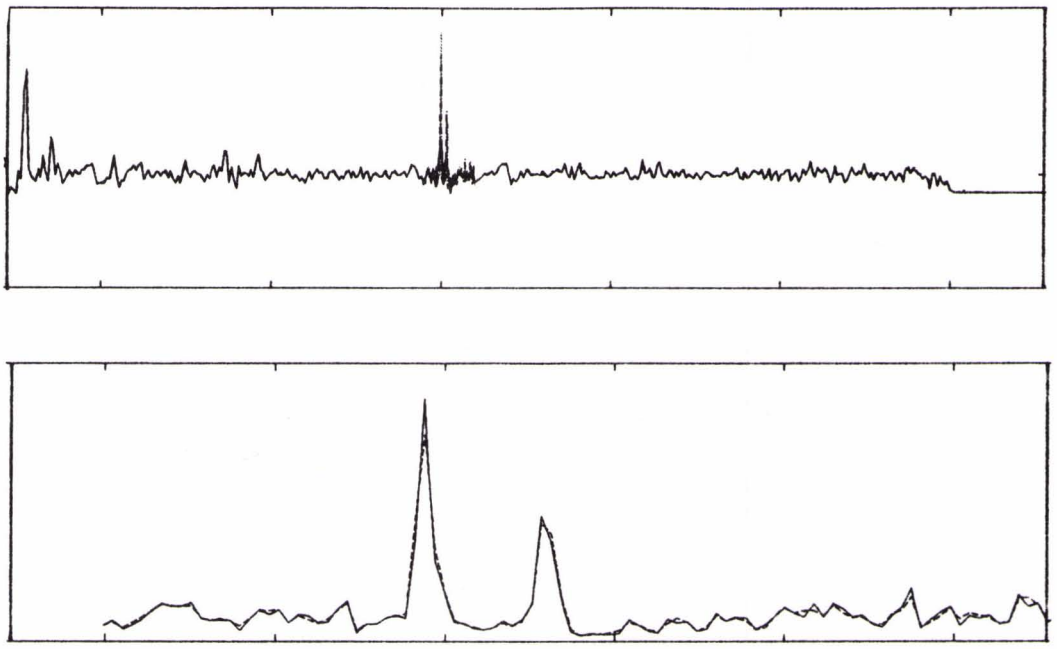

Fig. 5.7: Pulse A sec/4B Hz, Matched-Filter-Integrator and Split-Spectrum, Frequency cells B Hz

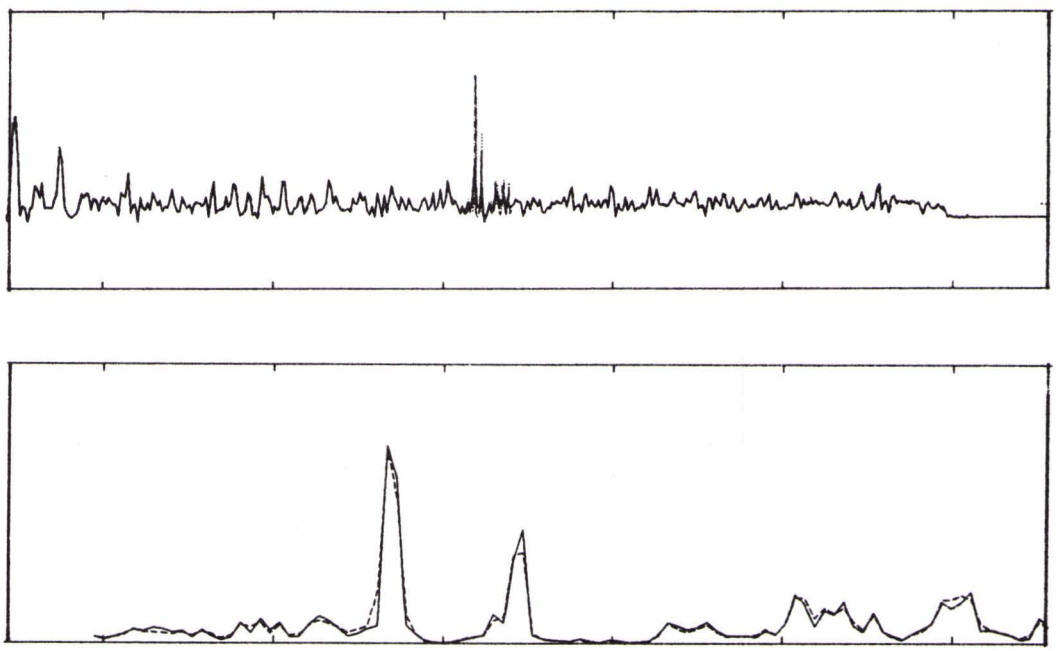

Fig. 5.8: Pulse A sec/B Hz, Matched-Filter

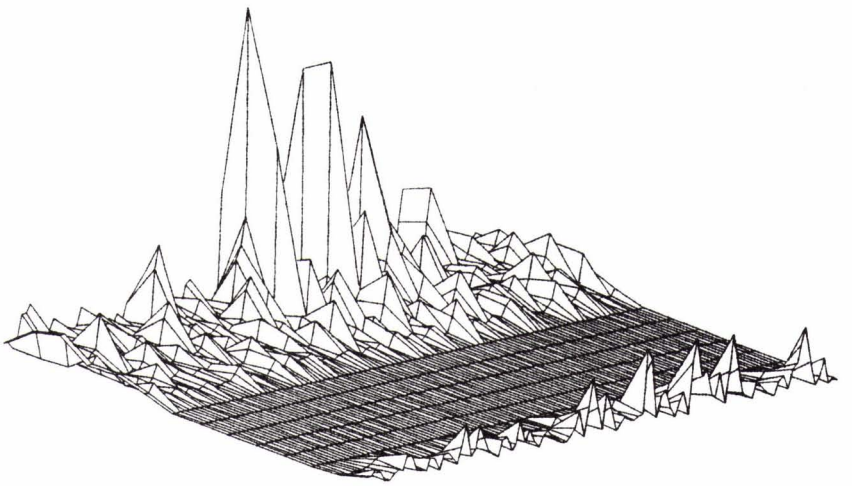

Noise and Reverberation Fluctuation over Frequency

Fig. 5.9: Pulse A sec/4B Hz, Frequency cells B Hz

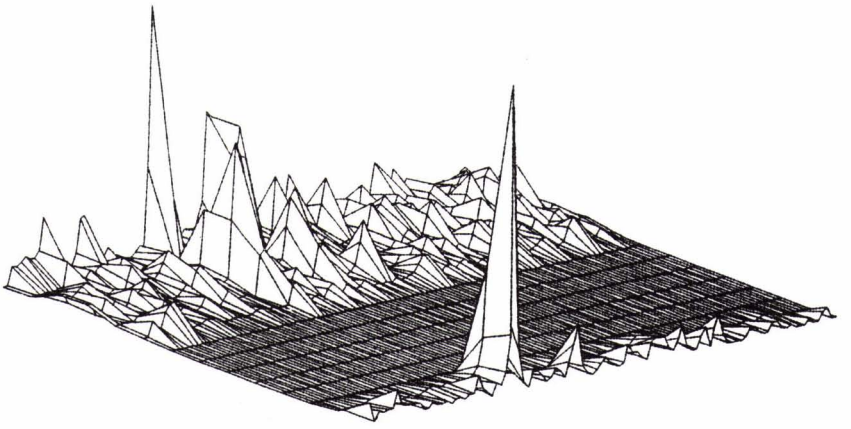

Noise and Reverberation Fluctuation over Frequency

Fig. 5.10: Pulse A sec/4B Hz, Frequency cells B Hz

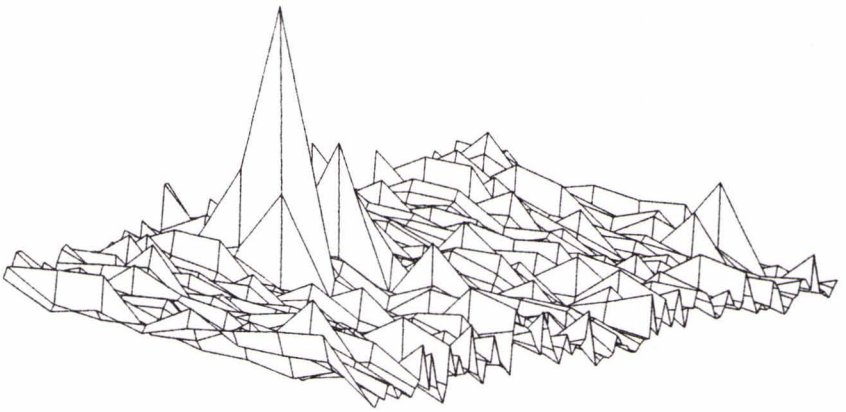

Fig. 5.11: Pulse A sec/4B Hz, Frequency cells B Hz

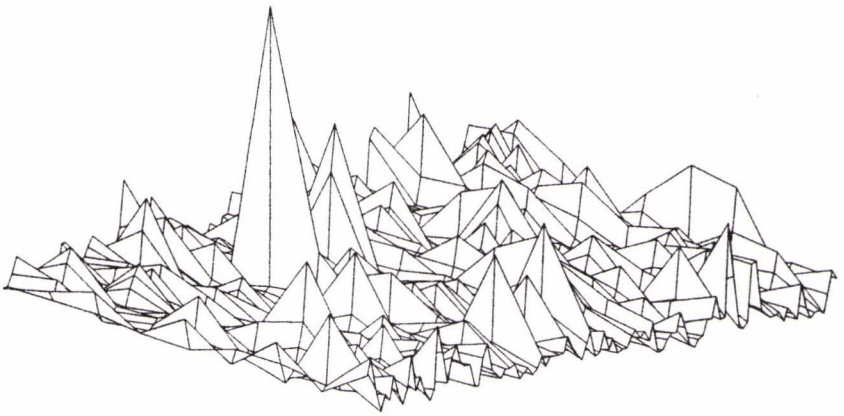

Fig. 5.12: Pulse A sec/B Hz

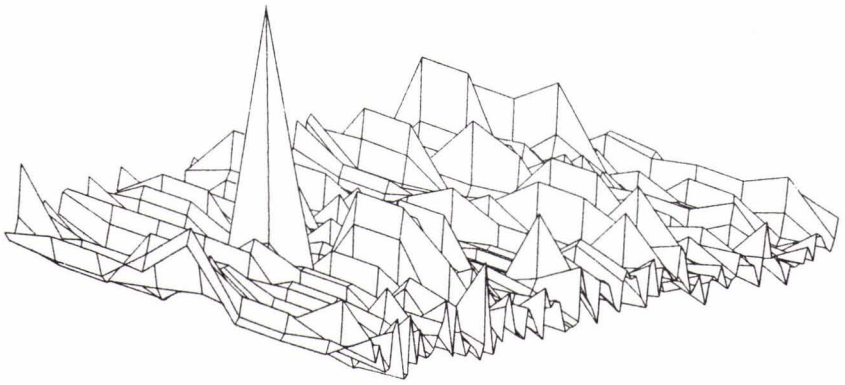

Fig. 5.13: Pulse A sec/4B Hz, Frequency cells B Hz

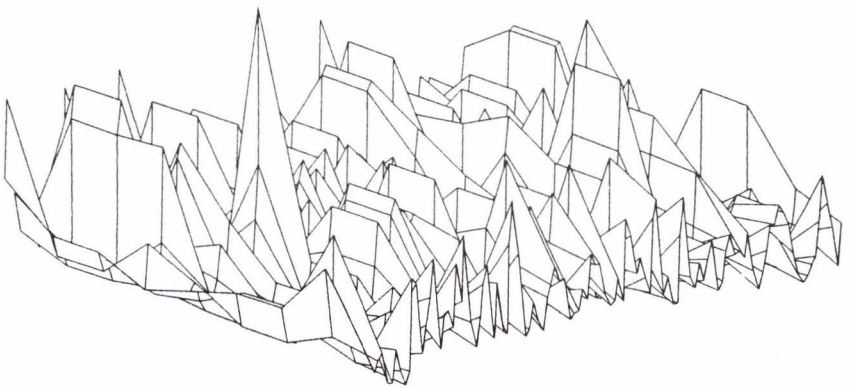

Fig. 5.14: Pulse A sec/B Hz

6 Conclusion

Two different signal processors for the detection of extended targets are presented, and a theoretical analysis of the bandwidth effects, including normalization, is given. Results of the processing of real data of wideband FM's are shown. The experimental results confirm the theoretical analysis.

7 References

[1] Helstrom, C. W. Detection probabilities for correlated Rayleigh fading signals. IEEE Transactions on Aerospace and Electronic Systems, 28, 1992: 259-267.
[2] Kantner, I. Exact detection probability for partially correlated Rayleigh targets. IEEE Transactions on Aerospace and Electronic Systems, 22, 1986: 184-195.
[3] Newhouse, V .L., Bilgutay, N. M., Saniie, J. and Furgason, E. S. Flaw-to-grain echo enhancement by split-spectrum processing. Ultrasonics, 1982.
[4] Papoulis, A. Probability, Random Variables, and Stochastic Processes. McGraw-Hill, 1991.
[5] Proakis J. G. Digital Communications. Mcgraw-Hill, 1989.
[6] Ries, S. and Roeckerath-Ries, M. TH. Signal processing for the detection of extended targets in noise and reverberation: theoretical aspects. Proceedings of the Institute of Acoustics, Vol 13 Pt. 9,1991: 59-66.
[7] Rohling, H. Radar CFAR thresholding in clutter and multiple target situations. IEEE Transactions on Aerospace and Electronic Systems , 19, 1983: 608-623.
[8] Shor, M. and Levanon, N. Performances of order statistics CFAR. IEEE Transactions on Aerospace and Electronic Systems, 27, 1991: 214-224.
[9] Van der Spek, G. A. Detection of a distributed target. IEEE Transactions on Aerospace and Electronic Systems, 7, No. 5, 1971: 922-931.
[10] Van der Spek, G. A. Detection of extended targets against noise and reverberation. Proc. Nato Advanced Study Institute, 1972.
[11] Van Trees, H. L. Detection, Estimation and Modulation Theory, Part III. John Wiley & Sons, New York, 1971.
[12] Whalen, A. D. Detection of Signal in Noise. Academic Press, 1971.